CHAPTER VII

INFLUENCE OF INITIAL SYSTEM PRESSURE ON THE DECOMPOSITION OF LiBH$_4$ AND MgH$_2$ MIXTURE

7.1 Abstract

The hydrogen desorption/absorption of the LiBH$_4$/MgH$_2$ mixture after milling for 5 h was investigated with different initial system pressures. The results showed that the initial system pressure played an important role in the reversibility of the LiBH$_4$/MgH$_2$ mixture. The stability of the hydrogen capacity in the subsequent desorption was improved with a higher initial system pressure. A possible reason was from the increase in the formation of MgB$_2$ and lower degree in the decomposition of both LiBH$_4$ to the amorphous phases of Li$_2$B$_{12}$H$_{12}$ and B and MgH$_2$ to Mg, during the hydrogen desorption. However, the higher initial system pressure increased the hydrogen desorption temperature. The desorption temperature was increased from 310°C for the sample decomposing under 0.1 MPa hydrogen pressure to 360°C for the other cases. That may be due to the need to increase the temperature to overcome the suppression of MgH$_2$ and LiBH$_4$ decomposition.
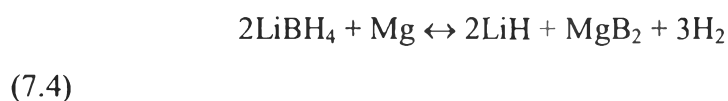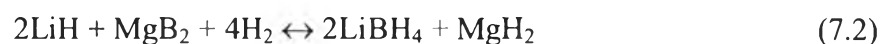
7.2 Introduction

Solid-state hydrides such as metal hydrides and complex hydrides are very attractive for storing a large amount of hydrogen because their safety and light weight compared to storing hydrogen in a high pressure gas tank or a cryogenic tank [1]. Complex hydrides have higher hydrogen desorption capacity than metal hydrides but they decompose at a very high temperature. Therefore, a major challenge for the complex hydrides is to lower the desorption temperature, enhance the reaction kinetics, and handle the reversibility issue [2-4].

LiBH$_4$ has been considered to be a potential hydrogen storage material because it has a very high hydrogen capacity of 18.4 wt% [5-6]. However, the decomposition of the material starts at a temperature higher than 400°C, Eq. (1). Practically, only 13.5 wt% hydrogen can desorb from the hydride as the remaining

hydrogen from LiH requires a temperature above 600°C. In addition, the reversibility of this material is not possible at moderate conditions.

$$LiBH_4 \rightarrow LiH + B + 1.5H_2$$

(7.1)
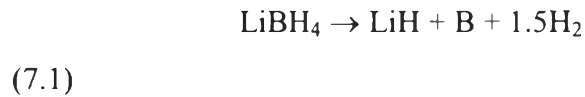
There are reports that mixing $LiBH_4$ with MgH_2 can improve hydrogen desorption/absorption properties. However, the maximum hydrogen desorption capacity is lowered to 11.4 wt%. Vajo et al. [7] first successfully recovered $LiBH_4$ by reacting MgB_2 with LiH and 3 mol% $TiCl_3$ to form $LiBH_4$ and MgH_2. They found that the reaction enthalpy was reduced by 25 kJ (mol of H_2)$^{-1}$ compared to $LiBH_4$, and 8-10 wt% hydrogen was obtained after two cycles of hydrogen desorption. They also reported that the absorption of the LiH/MgB_2 mixture took place with only one step for hydrogen absorption (Eq. (2)) and two steps for hydrogen desorption (Eqs. (3)-(4)). The results correspond with the reports from Bösenberg et al. [8] and Pinkerton et al. [9].

$$2LiH + MgB_2 + 4H_2 \leftrightarrow 2LiBH_4 + MgH_2 \qquad (7.2)$$

$$MgH_2 \leftrightarrow Mg + H_2$$

(7.3)

$$2LiBH_4 + Mg \leftrightarrow 2LiH + MgB_2 + 3H_2$$

(7.4)

Vajo et al. [7] reported that, under dynamic vacuum pressure, the first step of the hydrogen desorption from the $LiBH_4/MgH_2$ mixture was the decomposition of MgH_2 to Mg at 270-340°C, Eq. (3). For the second step of the hydrogen desorption at 380-440°C, melten $LiBH_4$ and spent MgH_2 from the first step decompose to LiH, amorphous boron, and Mg, without the formation of MgB_2 resulting in the loss of hydrogen capacity after the next hydrogen absorption.

However, applying a several bars of hydrogen gas during the hydrogen desorption, in the second step of hydrogen desorption, $LiBH_4$ would react with Mg to form LiH and MgB_2 and the reaction could be fully reversible [9-10]. The results imply that the hydrogen pressure seems to be an important factor to improve the hydrogen desorption/absorption of the $LiBH_4/MgH_2$ mixture. Nakagawa at el. [11] studied thermal analysis of the mixture of $LiBH_4$ and MgH_2 doped with $TiCl_3$ under 0.3 MPa inert gas flow and 0.5 MPa hydrogen gas flow by using DSC and XRD. The results show that during the hydrogen desorption at a temperature above 400°C, the $LiBH_4/MgH_2$ mixture was transformed to Mg, B, and LiH under the inert gas atmosphere, while MgB_2 and LiH were produced under the hydrogen gas atmosphere. Yang et al. [12] confirmed the formation of MgB_2 under different hydrogen pressures. At 400°C and 0.1 MPa hydrogen pressure, MgB_2 partially formed and the amount of MgB_2 was increased as the hydrogen pressure increased.

To have a complete picture, we further investigated the effects of initial system pressure including different gases and gas pressures on the hydrogen desorption/absorption properties of a 2:1 molar raio of $LiBH_4$ and MgH_2. The applied gas was hydrogen and argon with different initial pressures from 0.1 to 0.2 MPa. In addition, the phase transformation during the hydrogen desorption was also studied to elucidate the decomposition behavior of both $LiBH_4$ and MgH_2.

7.3 Experimental

To prevent oxygen and moisture contamination, all sample preparation was carried out in a nitrogen filled glove box. The starting materials, $LiBH_4$ (95%) and MgH_2 (90%), were purchased from Sigma-Aldrich and used without further purification. The mixture was prepared with ball milling (Retsch ball mill, Model S100) under 0.1 MPa nitrogen atmosphere at a speed of 300 rpm with a ball-to-powder ratio of 40:1 for 5 h. After the sample preparation, 0.5 g of a 2:1 molar ratio of $LiBH_4$ and MgH_2 was transferred into the Sievert's type apparatus. Before starting the hydrogen desorption, different initial system pressures, namely, 0.1, 0.15, and 0.2 MPa hydrogen pressures; and 0.2 MPa argon pressure, were set in the reactor, and

the hydrogen desorption was carried out from 25 to 450°C with a heating rate of 2°C min^{-1}. After that, the sample was compressed under 8.5 MPa hydrogen and 350°C for 12 h for hydrogen absorption. The same procedure was repeated to investigate the reversibility. The librerated hydrogen pressure in the system was measured by a pressure transducer (Cole Parmer, model 68073-68074) and used to calculate amounts of desorbed hydrogen. Only the increased pressure from the decomposition of LiBH$_4$/MgH$_2$, not including the initial system pressure, was used to calculate the amounts of desorbed hydrogen.

To understand the hydrogen desorption mechanism of the LiBH$_4$/MgH$_2$ mixture in different initial system pressures, the milled sample was subject to the desorption under isothermal condition, at contant temperatures of 350, 400, and 450°C before the phase transformation investigation by the XRD technique. The XRD analysis was carried out using a Rigaku X-ray diffractometer (Cu K_α, 40 kV, 30 mA) over the range of 20 to 80° at the room temperature.

7.4 Results and Disscussion

Hydrogen desorption profiles of the LiBH$_4$/MgH$_2$ mixture milled for 5 h under different desorption atmospheres are shown in Figs. 7.1-7.4. Fig. 7.1 shows the decomposition of the sample under 0.1 MPa hydrogen initial pressure, while Figs. 7.2 and 7.3 are under 0.15 and 0.2 MPa hydrogen initial pressures, respectively. In addition, the decomposition of the sample under 0.2 MPa argon initial pressure is shown in Fig. 7.4.
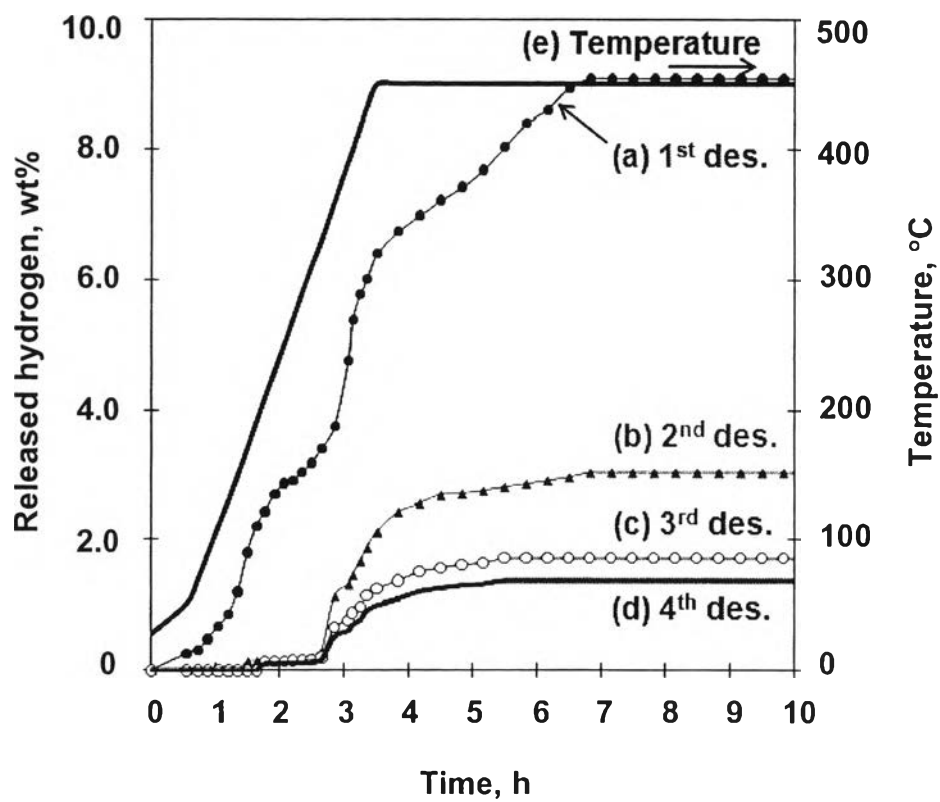
Figure 7.1 Hydrogen desorption profiles of the $LiBH_4/MgH_2$ mixture milled for 5 h after (a) first, (b) second, (c) third, (d) fourth hydrogen desorption, and (e) desorbed temperature under 0.1 MPa hydrogen initial pressure.
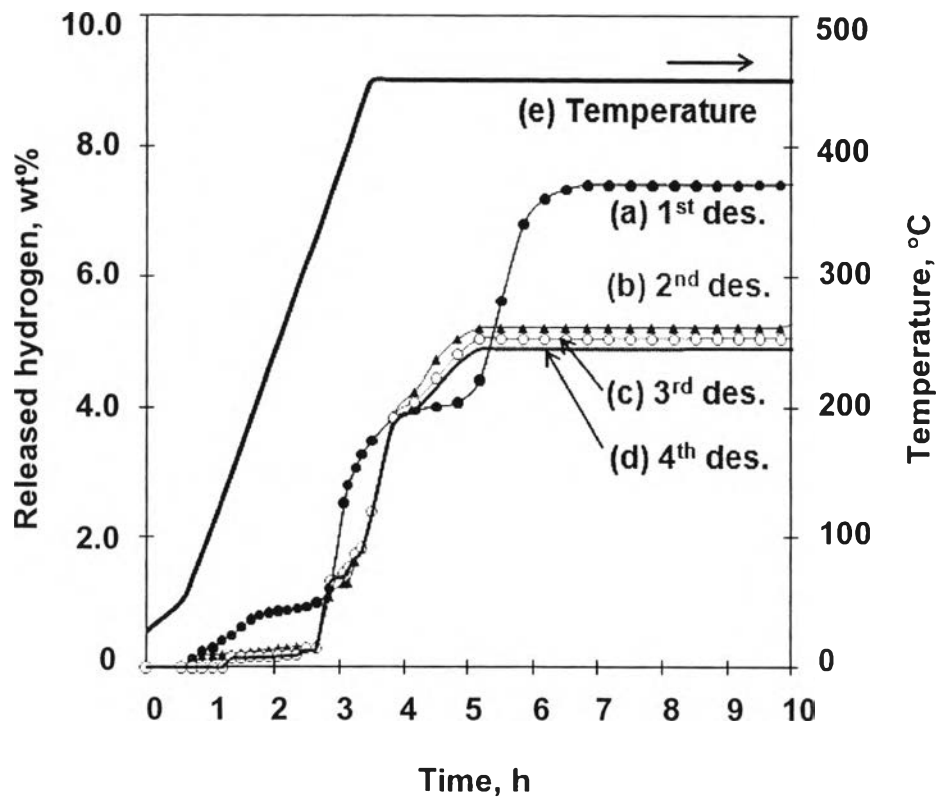
Figure 7.2 Hydrogen desorption profiles of the $LiBH_4/MgH_2$ mixture milled for 5 h after (a) first, (b) second, (c) third, (d) fourth hydrogen desorption, and (e) desorbed temperature under 0.15 MPa hydrogen initial pressure.

Figure 7.3 Hydrogen desorption profiles of the $LiBH_4/MgH_2$ mixture milled for 5 h after (a) first, (b) second, (c) third, (d) fourth hydrogen desorption, and (e) desorbed temperature under 0.2 MPa hydrogen initial pressure.
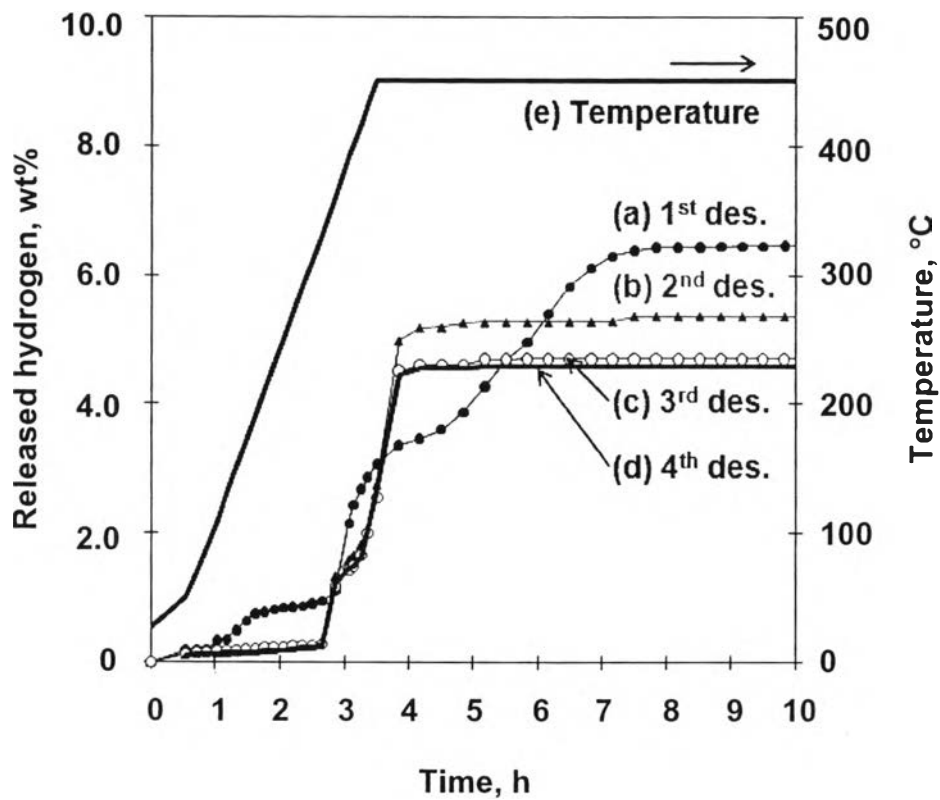
Figure 7.4 Hydrogen desorption profiles of the $LiBH_4/MgH_2$ mixture milled for 5 h after (a) first, (b) second, (c) third, (d) fourth hydrogen desorption, and (e) desorbed temperature under 0.2 MPa argon initial pressure.

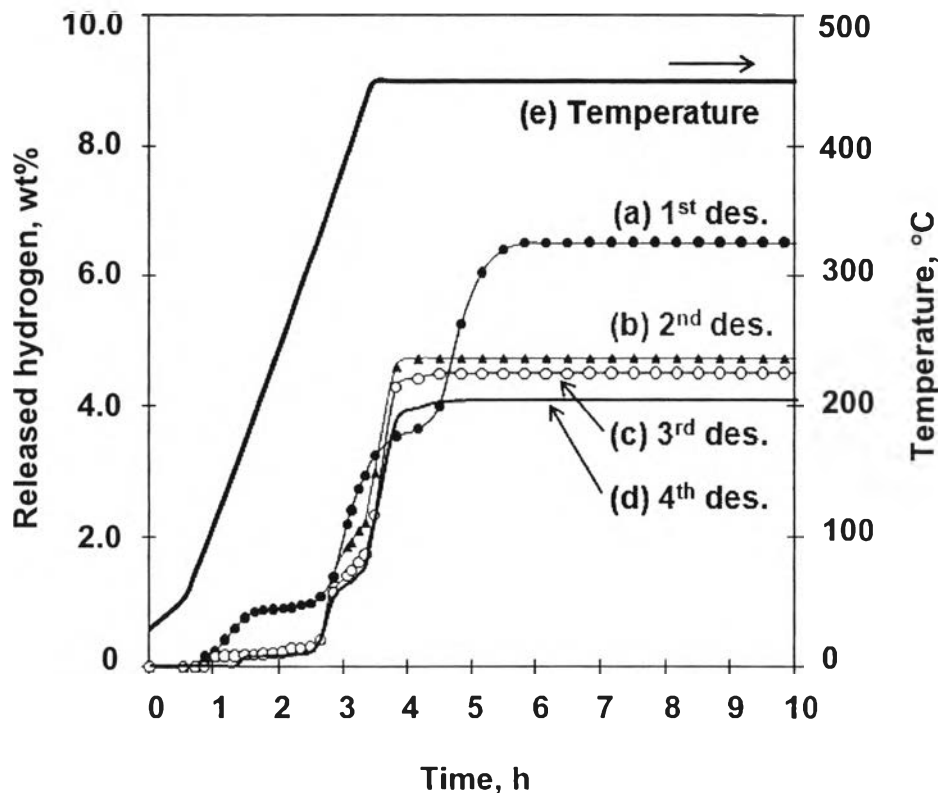For the first hydrogen desorption, in the first step, all samples start to release hydrogen at the same temperature, 50°C. In the second step, the hydrogen desorption under 0.1 MPa hydrogen pressure (Fig. 7.1(a)) starts at 310°C, which is lower than that under the other initial system pressures (360°C). In the third step, it seems that the initial system pressure does not affect the desorption temperature, and the hydrogen desorption takes place at 450°C for all cases. A possible reason for the higher desorption temperature in the second step of the desorption under 0.15 and 0.2 MPa hydrogen pressures and 0.2 MPa argon pressure may be from the higher initial pressure in the system resulting in the suppression of $LiBH_4$ and MgH_2 decomposition. Hence, a high temperature is needed for the sample to decompose. Separate experiments were carried out to confirm the effects of an initial system pressure on the decomposition behavior of $LiBH_4$ and MgH_2. Figs. 7.5 and 7.6 show

the decomposition of $LiBH_4$ and MgH_2 under 0.1 and 0.2 MPa hydrogen pressures, respectively. It was found that, with the applied initial system pressures, the hydrogen desorption temperatures of $LiBH_4$ and MgH_2 increase. For the first step, the hydrogen desorption temperatures from $LiBH_4$ under 0.1 and 0.2 MPa hydrogen pressures are the same at 50°C. For the second step, $LiBH_4$ decomposing under 0.1 MPa hydrogen pressure releases hydrogen at 380°C, which is lower than that under 0.2 MPa hydrogen pressure about 10°C. In the case of MgH_2, the sample decomposing under 0.1 MPa hydrogen pressure shows the incubation period at 50°C in the first step and significantly releases hydrogen at 300°C in the second step. However, MgH_2 decomposes under 0.2 MPa hydrogen pressure in one step at 340°C. The above result implies that the hydrogen desorption in the third step of the $LiBH_4/MgH_2$ mixture may be from a reaction between spent $LiBH_4$ and MgH_2 from the second step.

Figure 7.5 Hydrogen desorption profiles of (a) $LiBH_4$, (b) MgH_2, and (c) desorbed temperature after the first hydrogen desorption under 0.1 MPa hydrogen initial pressure.
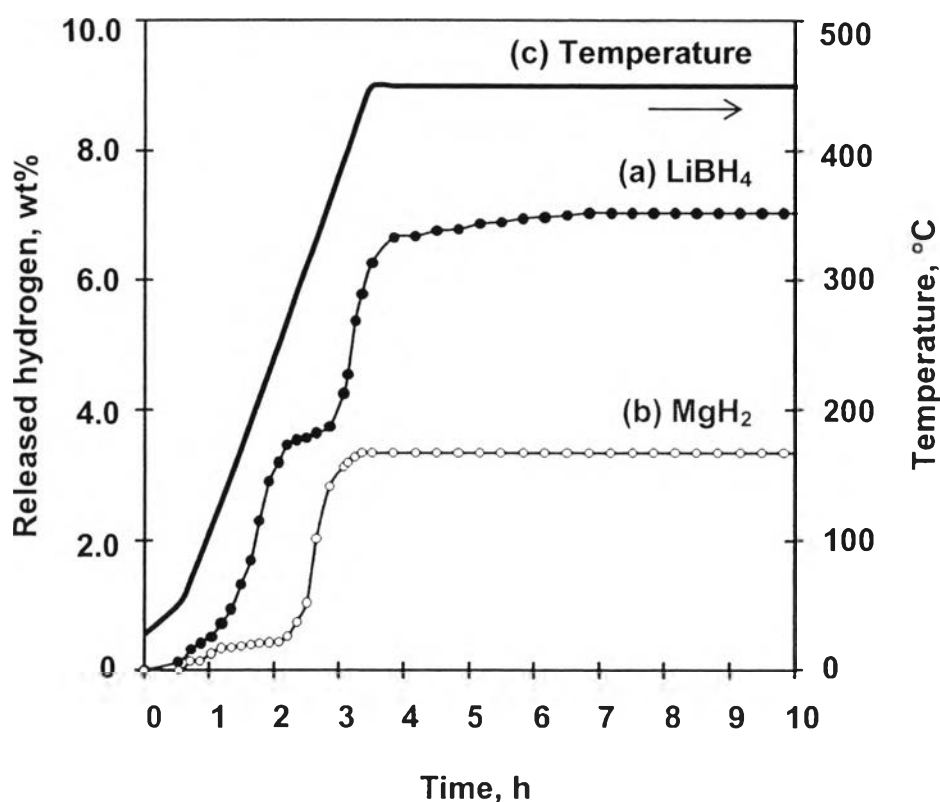
Figure 7.6 Hydrogen desorption profiles of (a) $LiBH_4$, (b) MgH_2, and (c) desorbed temperature after the first hydrogen desorption under 0.2 MPa hydrogen initial pressure.
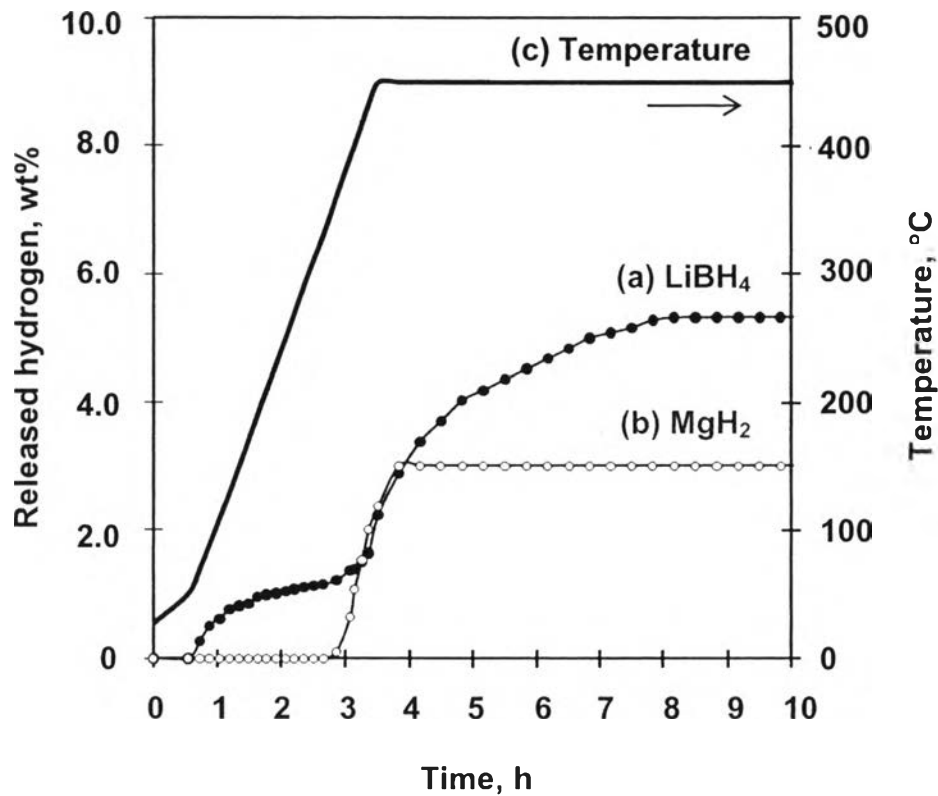
Table 7.1 Amounts of hydrogen from the $LiBH_4/MgH_2$ desorption in different initial system pressures

Initial system pressure	Hydrogen desorption capacity / wt%			
	1st des.	2nd des.	3rd des.	4th des.
0.1 MPa hydrogen pressure	9.0	3.0	1.7	1.3
0.15 MPa hydrogen pressure	7.4	5.3	5.0	4.9
0.2 MPa hydrogen pressure	6.5	5.3	4.7	4.6
0.2 MPa argon pressure	6.5	4.7	4.6	4.1

For the hydrogen desorption capacity in the first step of the first desorption or the *shoulder* (Figs. 7.1-7.4(a)), the sample decomposing under 0.1 MPa hydrogen pressure releases about 3.0 wt% hydrogen, which is higher than that under the other pressures, 1.0 wt% hydrogen. Comparison between the decomposition of $LiBH_4$ and MgH_2 under 0.1 and 0.2 MPa hydrogen pressures in Figs. 7.5 and 7.6 shows that the lower of the shoulder of the mixture is due to the lower degree in the decomposition of $LiBH_4$ and MgH_2, which may result from the initial system pressure. However, the lower amount of hydrogen in the first step is mainly from the decomposition of $LiBH_4$ because the released hydrogen of $LiBH_4$ decreases from 3.5 wt% under 0.1 MPa hydrogen pressure to 1.7 wt% under 0.2 MPa hydrogen pressure. In the second step, the highest cummulative released hydrogen of 7.2 wt% is from the sample decomposing under 0.1 MPa hydrogen pressure. The amount of released hydrogen drops to 4.0 wt% when the sample decomposes under 0.15 MPa hydrogen pressure. Further decrease in the hydrogen released can be observed when the decomposition takes place under 0.2 MPa hydrogen and argon initial pressures. For the total amounts of hydrogen, in the third step, the decomposition of the $LiBH_4/MgH_2$ sample under 0.1 MPa hydrogen pressure releases the highest amount of hydrogen. From Figs. 7.1-7.4(a) and Table 7.1, approximately 9.0, 7.4, 6.5, and 6.5 wt% hydrogen are released from the decomposition under 0.1, 0.15, 0.2 MPa hydrogen pressures, and 0.2 MPa argon pressure, respectively. Again, the sample decomposing under the lowest initial system pressure desorbs the highest amount of hydrogen, while the samples decomposing under the same amount of initial system pressure release the same amount of hydrogen. It implies that different types of initial system pressure hardly affect the total amount of released hydrogen. However, the hydrogen desorption kinetics in the third step of the sample decomposed under 0.2 MPa argon pressure (Fig. 7.4(a)) is faster than that under 0.2 MPa hydrogen pressure (Fig. 7.4(b)).

The effect of initial system pressure on the total hydrogen capacity of the $LiBH_4/MaH_2$ sample is further explained from the decomposition of both $LiBH_4$ and MgH_2 in Figs. 7.5 and 7.6. The figures confirm that the decrease in the total hydrogen desorption capacity is mainly from the suppression of $LiBH_4$, particularly in the first step. The decomposition of $LiBH_4$ under 0.2 MPa hydrogen pressure

releases approximately 5.3 wt% hydrogen, or 25% lower than that from the decomposition under 0.1 MPa hydrogen pressure (7.0 wt% hydrogen). Interestingly, the total amount of released hydrogen (1.7 wt% hydrogen) is quite similar to that in the first step (1.8 wt% hydrogen). Therefore, it can be concluded that the lower total released hydrogen is due to the lower extent in the decomposition of $LiBH_4$ in the first step. On the other hand, the total amount of hydrogen desorption of MgH_2 is nearly the same, 3.3 and 3.0 wt% hydrogen, for the sample decomposing under 0.1 and 0.2 MPa hydrogen pressures, respectively. In addition, the decrease in the amount of hydrogen is also dictated by the equilibrium pressure of the system. That is the higher the initial system pressure, the lower the hydrogen partial pressure desorbs from the mixture.

From Figs. 7.1-7.4, in the subsequent desorption, all cases result in the two-step hydrogen desorption. The sample decomposing under 0.1 MPa hydrogen starts to release hydrogen at 320°C for the first step and 405°C for the second step, while the samples decomposing under a higher desorbed pressure liberate hydrogen at the same temperature of 330 and 420°C for the first and the second step, respectively. The *shoulder* or the released hydrogen in the first step of the first hydrogen desorption does not appear in the subsequent desorption because the shoulder is the hydrogen decomposition induced from the ball-milling process [13]. The total amounts of desorbed hydrogen in each cycle are also shown in Table 7.1. For the second hydrogen desorption, the total hydrogen desorption capacity of the sample decomposing under 0.1 MPa hydrogen pressure is significantly reduced to 3.0 wt% or about 66.7% lower than that from the first hydrogen desorption. The total hydrogen desorption capacity is further reduced to 1.3 wt% after the fourth hydrogen desorption. For the samples decomposing under higher hydrogen system pressures of 0.15 and 0.2 MPa, they release the same amounts of hydrogen at 5.3 wt% in the second hydrogen desorpton, which is lower than that from the first hydrogen desorption about 28.4 and 18.5%, respectively. Although the amounts of released hydrogen under 0.2 MPa argon and hydrogen pressure are the same for the first hydrogen desorption, interstingly, in the second desorption, the total amount of desorbed hydrogen under the argon pressure (4.7 wt%) is lower than that under the

hydrogen pressure (5.3 wt%). At the fourth desorption, the sample decomposing under the hydrogen pressure seems to be able to maintain its reversible capacity compared to that under the argon pressure. All in all, the results indicate that, at a higher initial system pressure, the sample could maintain its reversibility capacity. That is probably because the initial system pressure suppresses the decomposition of MgH_2 to Mg resulting in the lower extent in the formation of MgO, which hinders the hydrogen absorption of LiH and MgB_2 [14-15]. In addition, the initial system pressure can lower the decomposition extent of $LiBH_4$ to amorphous structures (such as B and $Li_2B_{12}H_{12}$) before the reaction between $LiBH_4$ and MgH_2. That, in turn, prevents the amorphous phase formation from the interaction between the samples [16]. However, the lower amount of desorbed hydrogen of the sample decomposing under the argon pressure may be because argon is an inert gas, and it does not affect the partial pressure of hydrogen in the reaction (Eqs. (7.3)-(7.4)).

Fig. 7.7 shows the presence of LiH, MgB_2, Mg, and MgO indicating the incomplete hydrogen absorption to form the starting materials, $LiBH_4$ and MgH_2; hence, the lower amount of released hydrogen in the subsequent desorption is obtained. LiH, MgB_2, and Mg are the desorption products from the desorption of the $LiBH_4/MgH_2$ mixture, while MgO, which is difficult to reduce to MgH_2 under mild conditions, is the product between Mg and impurities in the system [17]. A possible reason for the significant lower desorbed hydrogen amount in the subsequent cycles of the sample decomposing under 0.1 MPa hydrogen may be from the presence of the Mg phase, which indicates insufficient hydrogen for the absorption. On the other hand, from the decomposition under 0.2 MPa hydrogen, the higher intensity of $LiBH_4$ and MgH_2 can be seen (Fig. 7.7(c)), and that may explain why a higher hydrogen amount was obtained in the subsequent desorption.
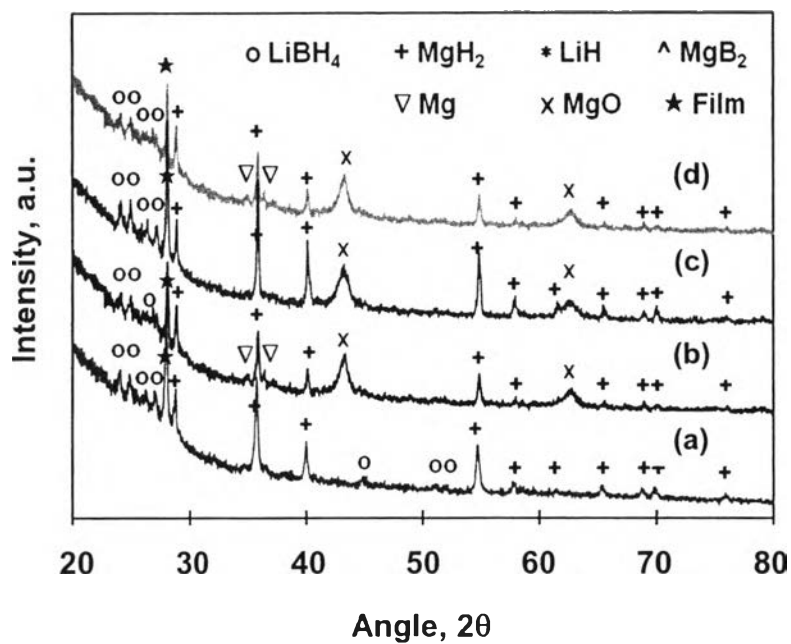
Figure 7.7 XRD patterns of the LiBH₄/MgH₂ mixture after (a) ball-milling for 5 h and after hydrogen absorption under 8.5 MPa hydrogen and 350°C for 12 h with different initial system pressures of (b) 0.1, (c) 0.2 MPa hydrogen pressures, and (d) 0.2 MPa argon pressure.

To understand the hydrogen desorption mechanism of the LiBH₄/MgH₂ mixture decomposing under different conditions, the phase transformation of the samples after the hydrogen desorption at constant temperatures of 350, 400, and 450°C was exaimined by the XRD technique. The results are shown in Fig. 7.8.
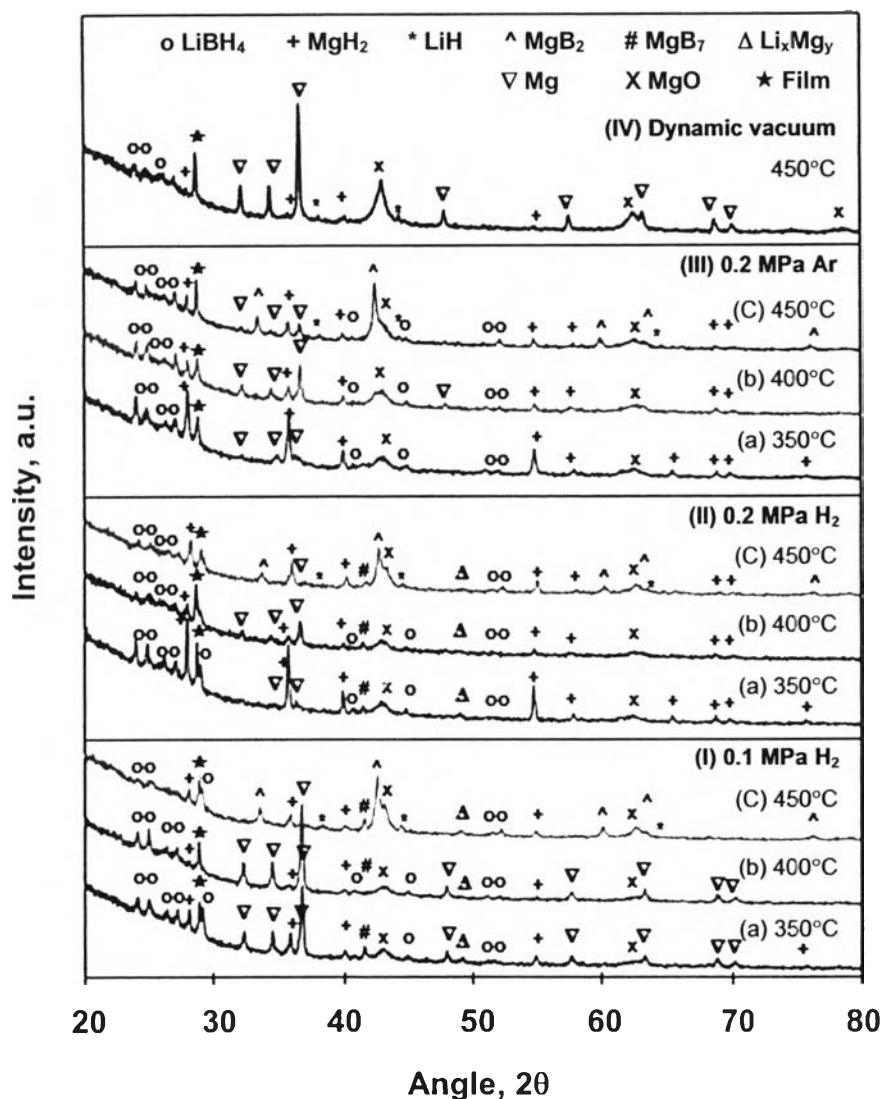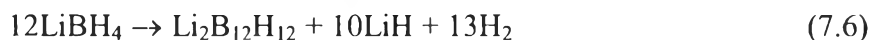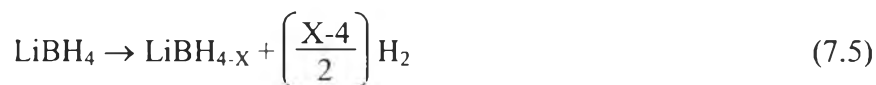
Figure 7.8 XRD patterns of the $LiBH_4/MgH_2$ mixture milled for 5 h after hydrogen desorption under (I) 0.1, (II) 0.2 MPa hydrogen pressures, (III) 0.2 MPa argon pressure at different desorption temperatures (a) 350, (b) 400, and (c) 450°C, and (IV) dynamic vacuum pressure at 450°C.

At 350°C, the sample decomposing under 0.1 MPa hydrogen pressure (Fig. 7.8(I)(a)) shows the higher intensity of the Mg phase than the sample decomposing under 0.2 MPa hydrogen (Fig. 7.8(II)(a)) and argon pressures (Fig. 7.8(III)(a)) This indicates that MgH_2 already decomposes to Mg at a temperature lower than 350°C for the sample decomposing under 0.1 MPa hydrogen pressure, while the sample decomposing under 0.2 MPa hydrogen and argon pressures, some MgH_2

decomposes to Mg at 350°C. The decomposition of MgH_2 is shown in Eq. (7.3). In the case of $LiBH_4$, the decomposition starts at a temperature lower than the theoretical one (380-420°C) because the use of ball-milling in the sample preparation may partially destabilize the sample. Interestingly, the extent of the $LiBH_4$ decomposition in the sample under 0.1 and 0.2 MPa hydrogen pressures is higher than that under 0.2 MPa argon pressure. That may be because the inert gas may hinder the decomposition of $LiBH_4$ before the onset temperature. The desorption products of $LiBH_4$ at 350°C include $LiBH_{4-x}$ (Eq. (7.5)) [5-6], $Li_2B_{12}H_{12}$, and B (Eqs. (7.6)-(7.7)) [16,18-22], which cannot be detected by the XRD analysis because $LiBH_{4-x}$, $Li_2B_{12}H_{12}$, and B are an amorphous structure. However, the decomposition of $LiBH_4$ can be confirmed by the formation of MgB_7.

$$LiBH_4 \rightarrow LiBH_{4-x} + \left(\frac{X-4}{2}\right) H_2 \tag{7.5}$$

$$12LiBH_4 \rightarrow Li_2B_{12}H_{12} + 10LiH + 13H_2 \tag{7.6}$$

$$Li_2B_{12}H_{12} \rightarrow 2LiH + 12B + 5H_2 \tag{7.7}$$

According to the DFT calculation, using a large amount of $LiBH_4$ will tend to form the product of MgB_7 rather than MgB_2, Eq. (7.8) [23]. The decomposition of $LiBH_4$ in the sample under 0.1 and 0.2 MPa hydrogen pressures indicates that the rich phase of B reacts with Mg and forms MgB_7 as a product. In addtion, some Li and Mg may react together and form an alloy phase of Li_XMg_Y [24].

$$7LiBH_4 + MgH_2 \rightarrow MgB_7 + 7LiH + 11.5H_2 \tag{7.8}$$

At 400°C, both $LiBH_4$ and MgH_2 in all samples (Fig. 7.8(I)-(III)(b)) further decompose to $LiBH_{4-x}$, $Li_2B_{12}H_{12}$, B, and Mg. The higher intensity of the Mg phase and the lower intensity of the remaining MgH_2 phase in the sample decomposing under 0.1 MPa hydrogen pressure indicate the higher extent of MgH_2 decomposition resulting in the higher desorbed hydrogen amount than the other samples, which

corresponds with the results in Figs. 7.1-7.4(a). For $LiBH_4$, after the desorption at 400°C, its intensity is lower than that at 350°C. In addition, the observation is the same regardless the initial system pressures. The results indicate the continued decomposition of $LiBH_4$ at 400°C. However, there is no formation of the LiH phase.

At 450°C, $LiBH_4$ and Mg in all samples start to react together and form the LiH and the MgB_2 phases, Eq. (7.4). The higher intensity of the LiH and the MgB_2 phases and the lower intensity of the $LiBH_4$ and the MgH_2 phases in the sample decomposing under 0.1 MPa hydrogen pressure indicate the higher degree of hydrogen desorption than the other samples resulting in the higher desorbed hydrogen amount. In addition, the higher intensity of the remaining Mg in the sample decomposing under 0.2 MPa argon pressure implies a lower extent of the reaction between $LiBH_4$ and Mg. Hence, the sample decomposing under 0.2 MPa argon pressure releases a lower desorbed hydrogen amount than the other samples.

To clarify the effect of pressure on the hydrogen desorption behaviors of the $LiBH_4/MgH_2$ mixture, the initial desorption pressure was changed to a dynamic vacuum, which has no accumulated hydrogen desorption pressure in the system. The XRD characterization of the sample after the hydrogen desorption at 450°C is shown in Fig. 7.8(IV). The result shows that only the Mg phase is formed without the MgB_2 phase. This indicates that the initial hydrogen pressure in the system contributes to the formation of MgB_2, which is believed to be responsible for the reversibility of the sample [10].

7.5 Conclusions

The initial system pressure affects the hydrogen desorption behavior of the $LiBH_4/MgH_2$ mixture milled for 5 h. For the desorbed hydrogen amount, the total amount from the first desorption is reduced from 9.0 wt% in the sample decomposing under 0.1 MPa hydrogen pressures to 6.5 wt% in the sample decomposing under 0.2 MPa hydrogen and argon pressure. The lower desorbed hydrogen amount is mainly influenced from the decomposition of $LiBH_4$. At the fourth hydrogen desorption, the sample decomposing under 0.1 MPa hydrogen

pressure is significantly reduced to 1.3 wt%, while the sample decomposing under 0.2 MPa hydrogen and argon pressures is reduced to 4.9 and 4.1 wt%, respectively. The reversibility of the system seems to increase with the initial system pressure. That is arguably because of the lower degree in the decomposition of $LiBH_4$ to form an amorphous phase, which causes the dead capacity of the sample and the lower Mg formation extent during the hydrogen desorption. The Mg phase could further react with the impurity in the system to form the MgO layer, which blocks the diffusion of hydrogen atoms to LiH and MgB_2 during the hydrogen absorption. The increase in the initial system pressure also increases the decomposition temperature of the sample. That is because the decomposition of $LiBH_4$ and MgH_2 is suppressed by the initial system pressure.

7.6 Acknowledgment

7.7 References

[1] L. Schlapbach, A. Züttel, Hydrogen-storage materials for mobile applications, Nature 414 (2001) 353-358.

[2] F. Schüth, B. Bogdanović, M. Felderhoff, Light metal hydrides and complex hydrides for hydrogen storage, Chem. Commun. (2004) 2249-2258.

[3] E. David, An overview of advanced materials for hydrogen storage, J. Mater. Proc. Technol. 162-163 (2005) 169-177.

[4] S. Satyapal, J. Petrovic, C. Read, G. Thomas, G. Ordaz, . The U.S. Department of Energy's National Hydrogen Storage Project: Progress towards meeting hydrogen-powered vehicle requirements, Catalysis Today 120 (2007) 250-256.

[5] A. Züttel, P. Wenger, S. Rentach, P. Suddan, Ph. Mauron, Ch. Emmenegger, $LiBH_4$ a new hydrogen storage materials, J. Power Sources 118 (2003) 1.

[6] A. Züttel, S. Rentsch, P. Fischer, P. Wenger, P. Sudan, Ph. Mauron, Ch. Emmenegger, Hydrogen storage properties of $LiBH_4$, J. Alloys Compd. 356-357 (2003) 515-520.

[7] J.J. Vajo, S.L. Skeith, F. Mertens, Reversible storage of hydrogen in destabilized $LiBH_4$, J. Phys. B 109 (2005) 3719.

[8] U. Bösenberg, S. Doppiu, L. Mosegaard, G. Barkhordarian, N. Eige, A. Borgschulte, T.R. Jensen, Y. Cernius, O. Gutfleisch, T. Klassen. M. Dornheium, R. Bormann, Hydrogen sorption properties of MgH_2-$LiBH_4$ composites, Acta Mater. 55 (2007) 3951.

[9] F.E. Pinkerton, M.S. Meyer, G.P. Meisner, M.P. Balogh, J.J. Vajo, Phase boundaries and reversibility of $LiBH_4$/MgH_2 hydrogen storage material, J. Phys. Chem. C 111 (2007) 12882.

[10] G. Barkhordarian, T. Klassen, M. Dornheim, R. Bormann, Unexpected kinetic effect of MgB_2 in reactive hydride composites containing complex borohydrides, J. Alloys Compd. 440 (2007) 18.

[11] T. Nakagawa, T. Ichikawa, N. Hanada, Y. Kojima, H. Fujii, Thermal analysis on the Li-Mg-B-H systems, J. Alloys Compd. 447 (2007) 306-309.

[12] J. Yang, A. Sudik, C. Wolverton, Destabilizing $LiBH_4$ with a metal (M = Mg, Al, Ti, V, Cr, or Sc) or metal hydride (MH_2 = MgH_2, TiH_2, or CaH_2), J. Phys. Chem. C 111(51) (2007) 19134-19140.

[13] P. Sridechprasat, Y. Suttisawat, P. Rangsunvigit, B. Kitiyanan, S. Kulprathipanja, Catalyzed $LiBH_4$ and MgH_2 mixture for hydrogen storage, Int. J. Hydrogen Energy 36(1) (2011) 1200.

[14] A. Zaluska, L. Zaluski, J.O. Ström-Olsen, Nanocrystalline magnesium for hydrogen storage, J. Alloys Compd. 288 (1999) 217.

[15] F.D. Manchester, D. Khatamian, Mechanisms for activation of intermetallic hydrogen absorbers, Mater. Sci. Forum 31 (1988) 261.

[16] J.H. Shim, J.H. Lim, S.U. Rather, Y-.S. Lee, D. Reed, Y. Kim, D. Book, Y.W. Cho, Effect of hydrogen back pressure on dehydrogenation behavior of LiBH$_4$-based reactive hydride composites, J. Phys. Chem. Lett. 1 (2010) 59-63.

[17] M. Zhu, H. Wang, L.Z. Ouyang, M.Q. Zeng, Composite structure and hydrogen storage properties in Mg-base alloys, Int. J. Hydrogen Energy 31 (2006) 253.

[18] N. Ohba, K. Miwa, M. Aoki, T. Noritake, S. Towata, Y. Nakamori, S. Orimo, A. Züttel, First-principles study on the stability of intermediate compounds of LiBH$_4$, Phys. Rev. B 74 (2006) 075110.

[19] S. Orimo, N. Nakamori, N. Ohba, K. Miwa, M. Aoki, S. Towata, A. Züttel, Experimental studies on intermediate compound of LiBH$_4$, Appl. Phys. Lett. 89 (2006) 021920.

[20] S-.J. Hwang, R.C. Bowman Jr., J.W. Reiter, J. Rijssenbeek, G.L. Soloveichik, J.C. Zhao, H. Kabbour, C.C. Ahn, NMR confirmation for formation of $[B_{12}H_{12}]^{2-}$ complexes during hydrogen desorption from metal borohydrides, J. Phys. Chem. C 112 (2008) 3164-3169.

[21] V. Ozolins, E.H. Majzoub, C. Wolverton, First-principles prediction of thermodynamically reversible hydrogen storage reactions in the Li-Mg-Ca-B-H system, J. Am. Chem. Soc. 131 (2009) 230-237.

[22] U. Bösenberg, D.B. Ravnsbæk, H. Hagemann, V. D'Anna, C.B. Minella, C. Pistidda, W. van Beek, T.R. Jensen, R. Bormann, M. Dornheim, Pressure and temperature influence on the desorption pathway of the LiBH$_4$-MgH$_2$ composite system, J. Phys. Chem. C 114 (2010) 15212-15217

[23] S.V. Alapati, J.K. Johnson, D.S. Sholl, Identification of destabilized metal hydrides for hydrogen storage using first principles calculations, J. Phys. Chem. B 110 (2006) 8769-8776.

[24] X.B. Yu, D.M. Grant, G.S. Walker, A new dehydrogenation mechanism for reversible multicomponent borohydride systems - the role of Li-Mg alloys, Chem. Commun. (2006) 3906-3908.